6자유도 측정 장치를 이용한 병렬 기구의 캘리브레이션 실험 결과

압둘 라우프*, 아슬람 퍼베즈, 김현호, 류제하 (광주과학기술원 기전공학과)

Experimental Results on Kinematic Calibration of Parallel Manipulator using 6 DOF Measurement Device

Abdul Rauf , Aslam Pervez, Hyunho Kim and Jeha Ryu (Department of Mechatronics, GIST)

Abstract

This paper presents kinematic calibration of parallel manipulators with partial pose measurements using a device that measures a rotation of the end-effector along with its position. The device contains an LVDT, a biaxial inclinometer, and a rotary sensor and facilitates automation of the measurement procedure. The device is designed in a modular fashion and links of different lengths can be used. The additional kinematic parameters required for the measurement device are discussed, kinematic relations are derived, and cost function is established to perform calibration with the proposed device. The study is performed for a six degree-of-freedom(DOF) fully parallel HexaSlide Mechanism(HSM). Experimental results show significant improvement in the accuracy of the HSM.

Key Words : HexaSlide Mechanism, Kinematic Calibration, Measurement Devices, Parallel Manipulators

1. Introduction

Kinematic calibration aims at the estimation of true values for a set of geometric parameters that relate the articular variables of a robot manipulator to the pose of its end-effector. Kinematic calibration is one of the central and core issue for experimental and autonomous robotics [1].

Schemes for kinematic calibration require redundant information that can be acquired by various methods. Fully autonomous calibration schemes acquire measurement information only from the internal sensors of the robot actuators and obtain the required redundant information by restraining mobility of the end-effector [2-5]. Semi-autonomous calibration schemes get the redundant information by adding extra sensors to the system [6-9]. The redundant information for classical calibration schemes is obtained by complete or partial measurement of the pose of the end-effector with some external sensors [10-15]. In addition, force relations can be used for calibration of parallel manipulators[16].

Autonomous calibration schemes provide economic, automatic, noninvasive, and fast data measurement. Fully autonomous calibration schemes by imposing constraints on the universal and spherical joints [2] and by imposing constraints on the end-effector [4] have been studied for 6 DOF fully parallel manipulators. Semi autonomous calibration schemes for Gough-Stewart platform have been proposed by adding two sensors at the universal joint of the alternate legs [6], and by using 5 extra sensors at the passive joints of one leg [8]. A combination of an extra sensor and a constraint can also be used to calibrate a general hexapod [9].

The autonomous calibration schemes also have their limitations. One important problem while implementing the fully autonomous calibration schemes is the back-drivability of the actuators. Restricting mobility of the end-effector requires some of the actuators to work in passive mode – not powered, yet providing sensor measurements. Errors in the nominal parameters appear as errors in the articular variables of the passive actuators, provided the actuators are back-drivable. Actuators with high reduction ratio may not be able to exhibit this desired feature. For the semi-autonomous calibration schemes, problem of adding the extra sensor(s) is not trivial and should be considered at the design stage. Also, additional sensors often require additional kinematic parameters.

Classical methods of calibration require measurement of complete or partial postures of the end-effector using some external measurement devices. Numerous devices have been used for calibration of parallel manipulators including a combination of electronic theodolites and standard measurement tapes [10], LVDT sensors [11], Laser displacement sensors [12], Double Ball Bar system [13,14], and inclinometers [15].

With complete measurement of the Cartesian pose, the calibration problem can be formulated in terms of inverse kinematic residuals. This results in a compact error model and a well-structured identification Jacobian and do not need solution of the forward kinematics. However, measuring all components of the Cartesian pose, particularly that of the orientation, can be difficult and expensive. The partial pose measurement schemes offer simpler experimental procedures. However, measuring only position or only orientation component(s) may result in poor identification [17].

For effective identification with simple experimental setup, Rauf et al. [18] proposed a measurement device that simultaneously measures the position and orientation components of the Cartesian pose of the end-effector. Their simulation results with the proposed device showed robust identification for a 6 DOF fully parallel HexaSlide type parallel manipulator. However, the device, being 5 DOF itself, restricts the end-effector to 5 DOF and requires one of the actuators to operate in passive mode while performing measurements. Passive actuators may introduce large errors because of poor back-drivability. This problem is solved by using an extendable link instead of a link with fixed length and measuring the length of the link. The measurement device of [18] is thus realized with an extendable link while employing a LVDT to measure the link extension. The inclusion of LVDT makes the device 6 DOF and therefore performing measurements do not require any passive actuators.

This paper presents experimental results for kinematic calibration with partial pose measurements using the above described measurement device. The experiments are performed for a 6 DOF fully parallel HexaSlide type parallel manipulator. The measurement device, however, is general and can be adapted for other parallel manipulators.

This paper is organized as follows: Section II and III, respectively, describe the HSM and the measurement device. Section IV presents the formulation for calibration. Experimental setup and results are discussed in section V. Section VI concludes the study.

2. The Mechanism

This section briefly introduces the parallel robot, HSM, to which the proposed calibration scheme is applied and presents its kinematics. Further details about the description and kinematics can be found in [18].

2.1 Description of the HSM

HSM is a 6 DOF fully parallel manipulator of PRRS type. Its geometric parameters are shown in fig. 1. The sliders are actuated along rail rails to control pose of the end-effector.

Pose (position and orientation) of the end-effector is represented in generalized coordinates by position of the mobile frame center in the base frame and three Euler angles.

$$\mathbf{X} = \begin{bmatrix} x & y & z & \psi & \theta & \phi \end{bmatrix} \quad (1)$$

The Euler angles are defined as: ψ rotation about the global X-axis, θ rotation about the global Y-axis and ϕ rotation about the rotated local z-axis. Orientation is thus given by $\mathbf{R} = \mathbf{R}_{Y,\theta}\mathbf{R}_{X,\psi}\mathbf{R}_{z,\phi}$. Note that the last rotation about the local z-axis is directly measured by the proposed measurement device as will be explained in section III.

2.1 Kinematics of the HSM

The inverse kinematics is solved in closed form, individually for each kinematic chain, as

$$\lambda = \mathbf{a}^{\mathrm{T}}\mathbf{A_0B} - \sqrt{\ell^2 - \left\|\mathbf{A_0B}\right\|^2 + \left(\mathbf{a}^{\mathrm{T}}\mathbf{A_0B}\right)^2} \quad (2)$$

The forward kinematics of the HSM may yield multiple solutions and is solved numerically using an iterative procedure [20].

2.2 Geometric Parameters of the HSM

Following are the minimum and independent parameters for a single kinematic chain of the HSM:

-- S joints' location – $\mathbf{B}$ – 3 parameters

-- Slider axis start point – $\mathbf{A_0}$ – 3 parameters

-- Direction vector along rail axis – $\mathbf{a}$ – 2 parameters

-- Link length – ℓ – 1 parameter

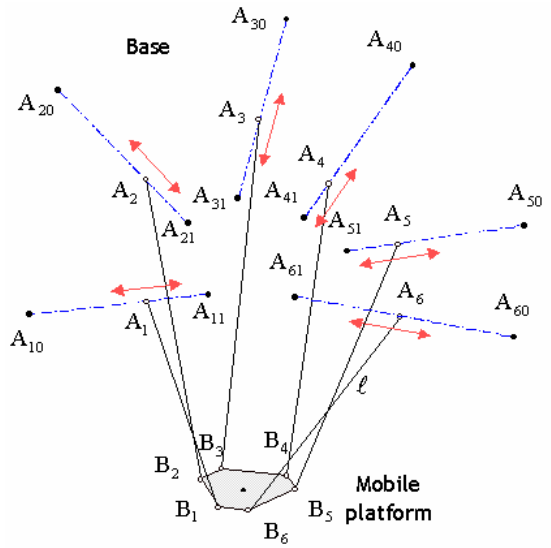

Fig. 1 Geometric parameters of the HSM

This makes 9 parameters for each chain and a total of 54 parameters for the HSM. Note that Fassi et al. [21] discussed the HSM under consideration, for their study on kinematic model for geometrical calibration of parallel robots and concluded that a total of 54 parameters are required, which is the same as considered in this study.

The details about HSM and the nominal values for its

geometric parameters can be found in [18,22].

3. The Measurement Device

This section presents a novel device for partial pose measurements of the end-effector using standard measurement gadgets. It describes the measurement device, develops its kinematics, and defines additional parameters of the device.

3.1 Description of the Measurement Device

Labeled 3D models of the components of the measurement device are shown in fig. 2 (left) along with a picture of the device while installed on HSM. It is a 6 DOF device and its architecture can be described as Universal-Prismatic-Sherical.

The measurement device consists of an extendable link with U joints on both sides. At one end, after the U joint, a rotary sensor is attached such that its axis of rotation passes through the U joint center. Note that U joint and rotary sensor form an equivalent S joint. The rotary sensor is coupled directly to the end-effector to measure rotation of the end-effector about the local z-axis. At the other end of the link, a flange is provided for mounting on the base. A LVDT and a biaxial inclinometer are mounted on the link to measure, respectively, its variable length and its tilt about two mutually perpendicular axes. Inclinometers are inertial devices that provide angular inclinations with respect to true vertical – the direction of gravity. The device is thus capable of measuring position of the end-effector using information of the biaxial inclinometer and the LVDT.

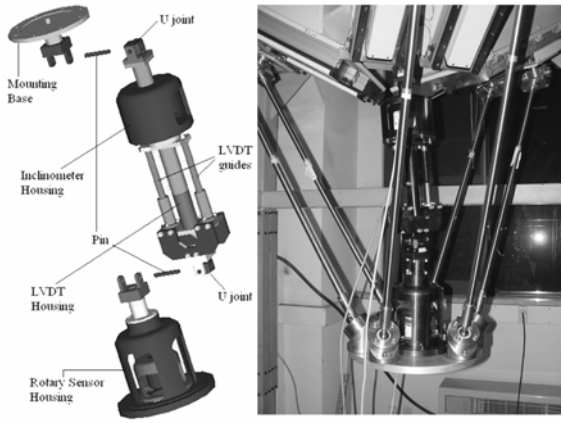

Fig. 2 The measurement device: CAD model and Fabricated system

The device is designed in a modular fashion. It has three distinct subassemblies that can simply be assembled by appropriately inserting pins as shown in fig. 2. The subassemblies are: the Mounting Base (at the top), the Link subassembly (in the middle), and the Encoder Housing (at the bottom). The Mounting Base is attached to a base plate at the frame of the HSM. It is fixed and supports the Link through a steel pin. The Encoder Housing is attached to the platform of the HSM. The encoder housing is also attached to the link through a steel pin. The Link subassembly is attached between the mounting base and the encoder housing subassemblies. The link subassembly houses a biaxial inclinometer and a LVDT. Referring to the fig. 2, the biaxial inclinometer is mounted in the upper cylindrical portion while the LVDT is installed inside the middle cylindrical link. The two columns, on each side of the cylindrical link housing the LVDT, are meant for supporting the load and contain bearings. The length of the measurement device, the distance between its U joint centers, needs to be selected carefully. The modular design of the measurement device allows links of various lengths. Therefore, the measurement device can be customized for manipulators of different sizes.

3.2 Frames and the Additional Parameters

For kinematic calibration of parallel manipulators, nominally, joint centers are modeled as points and links as lines. As shown in fig. 3, origins of the reference frames are defined with respect to the joint centers of the measurement device. The origin of the base frame, **O**, is located at the center of the U joint of the proposed measurement device near the base plate. The global Z-axis is directed along the direction of the gravity acceleration and the OXYZ forms a right-hand system. Global X-axis is defined parallel to the first measurement axis of the biaxial inclinometer. The origin of the mobile frame, **P**, is located at the center of the U joint near platform with the local z-axis, i.e. the z'-axis, being collinear with the rotational axis of the rotary sensor. The local x-axis and the local y-axis are defined parallel to the global X-axis and global Y-axis, respectively, at home position. Px'y'z' also forms a right-hand system.

Considering the reference frames as explained above, the following two parameters associated with the measurement device need to be considered as the additional kinematic parameters:

-- L_0 : The link offset of the measurement device.

-- γ : The angle between measurement axes of inclinometer.

The nominal values of L_0 and γ are 0.520 (m) and 90^o

3.3 Kinematics of the Measurement Device

Relations between the components of the Cartesian posture and the variables measured by the gadgets installed on the measurement device are developed in this subsection.

The position **P** of the end-effector with respect to **O** in terms of variables and parameters of the measurement device can then be given as

$$\begin{aligned} x &= -(L_0+L_m)(S\gamma C\gamma S\alpha(1-C\beta)-S\gamma S\beta C\alpha) \\ y &= -(L_0+L_m)(S\alpha-S\alpha C^2\gamma+S\alpha C\beta C^2\gamma+C\gamma S\beta C\alpha) \\ z &= -(L_0+L_m)(C\gamma S\beta S\alpha-C\beta C\alpha) \end{aligned} \quad (3)$$

where L_0 refers to the offset of the measurement device, L_m denotes the length measured by the LVDT (total length between the joint centers of the measurement device is the sum of two lengths), α is the inclination angle of link measured about global X-axis, and β is the inclination angle measured about an axis rotated at angle γ from the X-axis.

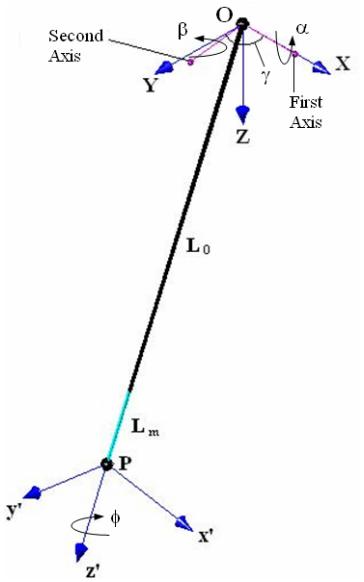

Fig. 3 Geometric parameters of the measurement device

3.4 Discussion

The main advantage of the developed measurement is its capability of complete parameter identification with partial pose measurements [18]. It also offers simple experimental setup and easy automation of the measurement procedure. Automatic motion to desired postures along with automatic data logging has been achieved using Simulink modules and ControlDesk layouts. Further, as the device is installed between the base and the end-effector of a parallel manipulator, it does not interfere with the working of the tool at the end-effector. The device, therefore, can be attached permanently to perform online compensation and/or help fast computation of forward kinematics.

The main disadvantage of the device lies in its tendency to reduce the working volume of a parallel manipulator. Parallel manipulators are known for their small workspace and further reduction in workspace can deteriorate effectiveness of calibration. It, therefore, may be required to customize the device for manipulator to be calibrated by making the workspace of the device equal to or larger than the workspace of the manipulator. Link offset, measurement range of LVDT, angular range of U joints, and measurement range of biaxial inclinometer can be optimally designed for required workspace. The modularity of the device facilitates its design.

4. Formulation for Calibration

4.1 Measurement Postures

With the measurement device attached, posture of the end-effector is restricted to a certain volume. The measurement postures and the trajectories traversed while moving from a posture to the next posture, therefore, need to be assured to lie within the measurement subspace. For each posture, articular variables are measured along with the inclination angles of the biaxial inclinometers, the rotation angle about the axis of the rotary sensor, and the displacement of the LVDT. Also, the commanded Cartesian pose needs to be recorded.

4.2 Cost Function

The *Calibration Index* is defined as the difference between the degree of sensing and the mobility of the robot [1]. Using the measurement device, 10 independent variables are measured for each pose of the 6 DOF end-effector. Thus, the calibration index for the proposed measurement device is 4, implying 4 independent constraints can be utilized for establishing cost function.

The cost function, as given in (4), is therefore established in terms of three position coordinates that can be computed by (3) and a single rotation angle that can be directly measured by a rotary sensor.

$$\Phi = \begin{bmatrix} x_m^i - x_c^i & y_m^i - y_c^i & z_m^i - z_c^i & \phi_m^i - \phi_c^i \end{bmatrix} \quad (4)$$

where the subscripts *m* and *c* correspond, respectively, to the measured and the computed values, and *i* indicate the number of measurement. Note that the computed values are obtained through forward kinematics. It is worthy to mention there are 4 constraints in (4) and thus the redundant information acquired through measurement device is fully utilized. Also note that the chosen cost function contains both the implicit (x, y, and z) and the explicit constraints. The purely explicit cost function, in terms of α, β, and ϕ can also be used [17]. However, the latter cost function requires a numerical solution for the system of (3), while the cost function of (4) solves the system of (3) in closed form. Results of computer simulations [22] affirm that (4) is more efficient.

4.3 Identification Procedure

The nonlinear identification problem of calibration is typically solved by gradient based optimization techniques. The function, "*lsqnonlin*", of Matlab optimization toolbox is used to perform identification while specifying bounds on the geometric parameters.

5. Experimental Setup and Results

This section describes the experimental setup used to obtain the measurement data and presents the experimental results.

5.1 Measurement Setup

5.1.1 Articular Variables

The articular variable of each kinematic chain is measured using an optical encoder coupled with its AC servomotor. Resolution of the encoder is 2500 counts per revolution, which is equivalent to a resolution of 4 micrometer considering pitch of the ball screws used. Taking into account the control error, resolution of the articular variables becomes about 15 micrometer. The measurements are acquired using DS3002 incremental encoder interface board of dSPACE [23].

5.1.2 Inclination Angles

Inclination angles, α and β, are measured by a biaxial inclinometer. LCF 2000/3000 type inclinometer of Jewell Instruments [24] is used for the purpose. The inclinometer provides measurements in the range ± 5 Volts for an angular range of $\pm$ 30 degrees. The inclinometer offers a resolution of 1 micro radian and its output voltage is measured using a high performance oscilloscope, Agilent Infiniium 54832D MSO. Also, for automation, output of inclinometer is acquired through two channels of the DS2002 ADC board of dSPACE.

Resolution and accuracy of the measurement device depends directly on the resolution and accuracy of the inclinometer. To fully exploit the resolution of inclinometer, the output signal is required to be measured precise to 10 micro Volts. In reality, measurements are performed with a precision of 100 micro Volts. Using (3), it can be seen that a precision of 10 micro Volts corresponds to a resolution of less than a micrometer in position components, while a precision of 100 micro Volts to a few (about 10) micrometers at an arbitrary pose.

5.1.3 Rotation Angle

The rotation angle, ϕ, is measured by an optical incremental encoder of BEI Technologies Inc. [25]. The encoder provides 128000 counts for a revolution that amounts to a resolution of about 10 seconds of arc. The measurement is acquired using a channel of 5-channel incremental encoder interface board from dSPACE, DS3001.

5.1.4 Length of the Link

The variable length of the link, L_m, is measured using a LVDT from Schaevitz Sensors, HCA 500 [26]. The device has a measurement range of $\pm$ 0.5 inches and offers a resolution of 1 micrometer. In reality, the obtained resolution was about 5 micrometers. A LVDT Panel Meter, PML1000-040, is used to provide excitation voltage to the LVDT and to display its output. For automatic data acquisition, analog voltage from the Panel Meter is also acquired using DS2002 ADC board.

5.2 Automation of Measurement Postures

Automation of calibration experiments requires automatic data acquisition, automatic motion, and automatic data logging. The acquisition of data for HSM and sensors is achieved through appropriate hardware components, as explained earlier, and is automatic. The automatic motion and automatic data logging is accomplished through a Simulink module and using the features of ControlDesk [27].

5.3 Experimental Results and Discussion

About 100 postures were measured with the setup discussed above. Note that for measurements, after commanding a posture, a delay was observed to let the transients diminish. The postures were measured both in the central workspace as well as at the boundaries of the workspace.

Fig. 4 shows the trend of the cost function, marked by a sharp initial decrease, which is typical for the identification. Figs. 5 and 6 compare errors in pose components, x and ϕ, before and after identification. Errors are represented by the distance of respective marks from datum (0-line), '●' for errors before calibration and '×' for errors after calibration. A significant decrease in the bias is obvious from figures. A similar trend was observed for errors in y and z components of pose, which can be seen in [22]. Table I compares mean and RMS values of errors before and after calibration. It also presents confidence intervals for mean values computed using Student distribution with 95% confidence level, computed as follows [28].

$$\bar{x} - \frac{st_\alpha}{\sqrt{N}} \prec \mu \prec \bar{x} + \frac{st_\alpha}{\sqrt{N}} \tag{5}$$

where $\bar{x}$ and s are the computed mean and standard deviation, μ is the estimated mean, t_α is a coefficient obtained from tables for required confidence level, and N refers to the number of data measurements.

From calibrated values, it can be observed that RMS values of pose errors are significantly improved. Also, bias is decreased for all of the measured pose components. Note that although the mean error along Y-axis before calibration is much higher than the other pose components, the mean after calibration is of the same order as of other pose components. This reflects robustness of the proposed calibration scheme with respect to initial errors. Interval estimates, after calibration, clearly show that bias is reduced. Also, since the confidence intervals after calibration are narrower, the results after calibration are more confined than before it. It, therefore, can be stated that the experimental results verify the validity and effectiveness of the proposed measurement device.

While experimental results show that the developed measurement device can be effectively used for calibration of parallel manipulators, its performance can be increased in number of ways. Link offset of the proposed measurement device was observed to be a bit longer, and therefore, measurements were performed in lower region

of manipulator's workspace. Decreasing link offset and employing LVDT of wider range can improve effectiveness of the developed measurement device. To achieve precision and high stiffness, the device is fabricated heavy, weighing about 11 Kg. Research can be extended for better design of the measurement device without compromising on accuracy.

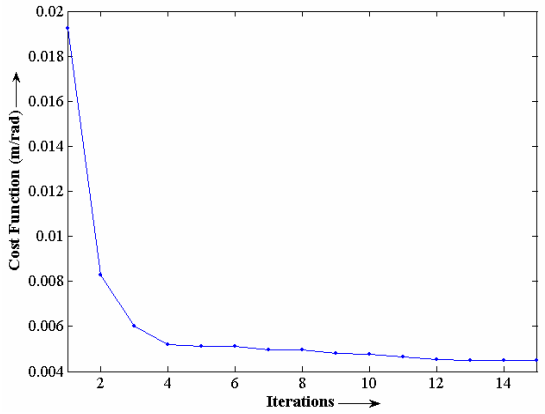

Fig. 4 Trend of the cost function

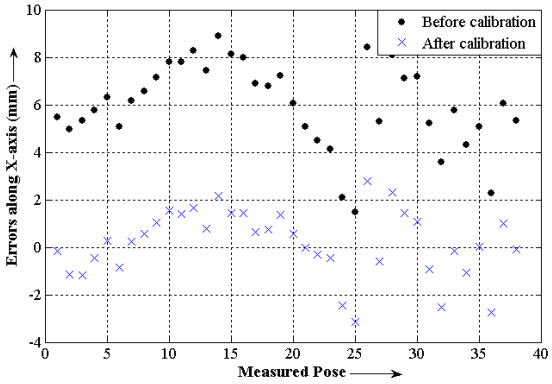

Fig. 5 Errors along X-axis.

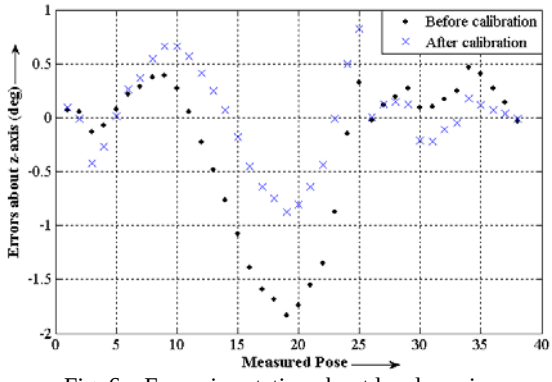

Fig. 6 Errors in rotation about local z-axis.

TABLE I

Error Comparison for Nominal and Calibrated Parameters

	x (mm)	y (mm)	z (mm)	ϕ (deg)
		RMS		
Nominal	6.31	34.84	3.75	0.76
Calibrated	1.60	3.61	0.90	0.42
		MEAN		
Nominal	6.00	-34.64	3.00	-0.27
Calibrated	0.20	-0.11	0.02	0.00
		ESTIMATED INTERVALS FOR MEAN		
Nominal	5.70~6.31	-35.2~34.0	2.65~3.35	-6.70~-2.82
Calibrated	-0.05~0.45	-0.68~0.45	-0.12~0.16	-1.15~1.14

6. Conclusion

A modular device for partial pose measurements of parallel manipulators is presented. The device contains standard gadgets including a LVDT and a biaxial inclinometer for measurement of position and an optical encoder for measurement of a rotation. The device offers a simple and automatic measurement procedure and can be used for online compensation. Experimental results show significant decrease of errors in the pose of end-effector. Therefore, the proposed measurement device can be effectively used for the calibration of parallel manipulators. Performance of the device can be improved by customizing the device for manipulator to be calibrated such that it does not reduce the workspace.

7. References

[1] J. M. Hollerbach, and C. W. Wampler, "The calibration index and taxonomy for robot calibration methods," The Int. Journal of Robotic Research, 15(6) 1996, pp. 573–591.

[2] W. Khalil, and S. Besnard, "Self calibration of Stewart-Gough parallel robots without extra sensors," IEEE Trans. on Robotics and Automation, 1999, pp. 1116–1121.

[3] P. Maurine, K. Abe, and M. Uchiyama, "Towards more accurate parallel robots," IMEKO-XV World Congress, Japan, 1999, Vol. X, pp. 73-80.

[4] J. Ryu, and A. Rauf, "A new method for fully autonomous calibration of parallel manipulators using a constraint link," AIM'01 conference, Italy, 2001, pp. 141-146.

[5] A. Rauf, and J. Ryu, "Fully autonomous calibration of parallel manipulators by imposing position constraint," IEEE Int. Conf. on Robotics and Automation, Seoul, 2001, pp. 2389-2394.

[6] H. Zhuang, and L. Liu, "Self-Calibration of a class of Parallel Manipulators," IEEE Int. Conf. on Robotics and Automation, 1996, pp. 994-999.

[7] H. Zhuang, “Self-calibration of parallel mechanisms with a case study on Stewart platforms,” IEEE Trans. on Robotics and Automation, 13(3), 1997, pp. 387-397.
[8] C. W. Wampler, J. M. Hollerbach, and T. Arai, “An implicit loop method for kinematic calibration and its application to closed-chain mechanisms,” IEEE Trans. on Robotics and Automation, 11(5) 1995, pp. 710-724.
[9] Y. J. Chiu, and M. H. Perng, “Self-calibration of a general hexapod manipulator with enhanced precision in 5-DOF motions”, Mechanism and Machine Theory, Vol. 39, Issue 1, 2004, pp. 1-23.
[10] H. Zhuang, J. Yan, and O. Masory, “Calibration of Stewart platforms and other parallel manipulators by minimizing inverse kinematic residuals,” Journal of Robotic Systems, 15(7), 1998, pp. 395-405.
[11] A. Nahvi, J. M. Hollerbach, and V. Hayward, “Calibration of parallel robot using multiple kinematic closed loops,” IEEE Int. Conf. on Robotics and Automation, 1996, pp. 407-412.
[12] P. Maurine, and E. Dombre, “A calibration procedure for the parallel robot Delta 4,” IEEE Int. Conf. on Robotics and Automation, 1996, pp. 975-980.
[13] H. Ota, T. Shibukawa, T. Tooyama, and M. Uchiyama, “Forward kinematic calibration method for parallel mechanism using pose data measured by a double ball bar system,” Proceedings of the Year 2000 Parallel Kinematic Machines Int. Conf., 2000, pp. 57-62.
[14] Y. Takeda, G. Shen, and H. Funabashi, “A DBB-based kinematic calibration method for in-parallel actuated mechanisms using a fourier series,” Proceedings of DETC’02: ASME 2002 Design Engineering Technical Conferences and Computer and Information in Engineering Conference, DETC2002/MECH-34345, 2002, pp. 1-10.
[15] S. Besnard, and W. Khalil, “Calibration of parallel robots using two inclinometers,” Proceedings of IEEE International Conference on Robotics and Automation, 1999, pp. 1758-1763.
[16] J. I. Jeong, D. Kang, Y. M. Cho, and J. kim, “Kinematic calibration for redundantly actuated parallel mechanisms,” Journal of Mechanical Design, Vol. 126, 2004, pp. 307-318.
[17] S. Besnard, and W. Khalil, "Identifiable parameters for parallel robots kinematic calibration," Proceedings of IEEE International Conference on Robotics and Automation, Seoul, 2001, pp. 2859-2866.
[18] A. Rauf, S. G. Kim, and J. Ryu, “Complete parameter identification of parallel manipulators with partial pose information using a new measurement device,” Robotica, vol. 22, 2004, pp. 689-695.
[19] A. Rauf, S. G. Kim, and J. Ryu, 2004, “A New Measurement Device for kinematic calibration of parallel manipulators,” DETC’04: ASME 2004 Design Engineering Technical Conferences & Computers & Information in Engineering Conference, DETC2004-57375, 2004, pp. 1-8.
[20] J. P. Merlet, Parallel Robots, Kluwer academic publishers, The Netherlands, 2000.
[21] I. Fassi, and G. Legnani, “Automatic identification of a minimum, complete and parametrically continuous model for the geometrical calibration of parallel robots,” Proc. of the Workshop on fundamental issues and future research directions for parallel mechanisms and manipulators, Canada, 2002, pp. 204-213.
[22] A. Rauf, “Kinematic calibration of parallel manipulators with partial pose information,” PhD Thesis, Department of Mechatronics, Gwangju Institute of Science and Technology, Republic of Korea, June 2005.
[23] dSPACE, http://www.dspace.de/ww/en/pub/home.htm
[24] Jewell Instruments, http://www.jewellinstruments.com
[25] BEI Technologies, Inc., http://www.bei-tech.com/
[26] Schaevitz Sensors, http://www.msiusa.com/schaevitz/
[27] ControlDesk, http://www.dspace.de/ww/en/pub/products/sw.htm
[28] C. J. Stone, “A course in statistics and probability,” Duxbury Press, Wadsworth Publishing Company (ITP), USA, 1996.